ACS APPLIED MATERIALS & INTERFACES

Research Article

www.acsami.org

Hydrogel-Based Microactuators with Remote-Controlled Locomotion and Fast Pb^{2+}-Response for Micromanipulation

Ying-Mei Liu,[†] Wei Wang,[†,*] Wei-Chao Zheng,[†] Xiao-Jie Ju,[†] Rui Xie,[†] Djamal Zerrouki,[§] Nan-Nan Deng,[†] and Liang-Yin Chu[†,‡,*]

[†]School of Chemical Engineering, Sichuan University, Chengdu, Sichuan 610065, P. R. China

[§]Department of Chemical Engineering, University of Ouargla, BP 511, Ouargla 30000, Algeria

[‡]State Key Laboratory of Polymer Materials Engineering, and Collaborative Innovation Center for Biomaterials Science and Technology, Sichuan University, Chengdu, Sichuan 610065, P. R. China

Supporting Information

ABSTRACT: Hydrogel-based microactuators that enable remote-controlled locomotion and fast Pb^{2+}-response for micromanipulation in Pb^{2+}-polluted microenvironment have been fabricated from quadruple-component double emulsions. The microactuators are Pb^{2+}-responsive poly(*N*-isopropylacrylamide-*co*-benzo-18-crown-6-acrylamide) microgels, each with an eccentric magnetic core for magnetic manipulation and a hollow cavity for fast Pb^{2+}-response. Micromanipulation of the microactuators is demonstrated by using them for preventing Pb^{2+}-leakage from microchannel. The microactuators can be remotely and precisely transported to the Pb^{2+}-leaking site under magnetic guide, and then clog the microchannel with Pb^{2+}-responsive volume swelling to prevent flowing out of Pb^{2+}-contaminated solution. The proposed microactuator structure provides a potential and novel model for developing multifunctional actuators and sensors, biomimetic soft microrobots, microelectromechanical systems and drug delivery systems.

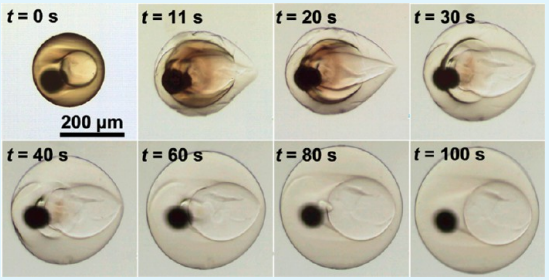

KEYWORDS: *microactuators, microgels, magnetic materials, microfluidics, molecular recognition, micromanipulation*

INTRODUCTION

Stimuli-responsive hydrogels, which can change their shape, size, or mechanical properties in response to stimuli such as temperature,[1−3] electric field,[4] pH,[4,5] humidity,[6] water gradient,[7] and chemical reaction,[8] are widely used for fabricating microactuators for micromanipulation such as thermo-driven moving, electric-field or pH-driven bending, and humidity or chemical-reaction-driven walking. Especially, responsive hydrogel systems that are capable of recognizing specific heavy metal ions are promising for developing microactuators for micromanipulation in heavy-metal-polluted microenvironment. Among those ions, lead(II) (Pb^{2+}) is one of the most abundant and toxic heavy metal pollutants, because of the long-term toxic effect resulted from its nonbiodegradability and unwanted accumulation in environment.[9] Even very low levels of lead exposure can cause renal and neurological damages, blood and brain disorders, and reproductive toxicity for humans, especially for infants and children.[10−12] Therefore, design and fabrication of hydrogel systems with Pb^{2+}-responsive shape or volume change characteristics as microactuators for micromanipulation in Pb^{2+}-polluted microenvironment is of both scientific and technological importance.

Crown ethers,[13−19] especially 18-crown-6, which are usually incorporated with acrylamides to realize Pb^{2+}-induced volume change due to the formation of supermolecular host−guest BCAm/Pb^{2+} complexes, are one of the most promising Pb^{2+}-responsive materials because of their selectivity and high complex efficiency.[20−22] By incorporation of thermo-responsive *N*-isopropylacrylamide (NIPAM)[23,24] with different contents of ion-recognizable benzo-18-crown-6-acrylamide (BC18A6m), a series of poly(NIPAM-*co*-B18C6Am) linear copolymers have been synthesized, which are found to be most sensitive to Pb^{2+} among different metal ions.[21] However, the poor mechanical strength and good water-solubility of these linear copolymers limit their application as microactuators. Molecular-recognition ion gating membranes have been fabricated by grafting linear poly(NIPAM-*co*-B18C6Am) copolymers onto the pore surfaces of porous membranes,[25−28] which enable controllable change of solution flux through the membrane in response to Pb^{2+} independent of other coexisting ions such as Ca^{2+}, Na^{+}, and Li^{+}.[28] Nevertheless, the linear poly(NIPAM-*co*-B18C6Am) copolymers that immobilized on membrane substrates restrict their flexible applications as freely movable actuators. Although cross-linked hydrogel films[29−34] and bulk hydrogels[21,35] of acrylamides and B18C6Am provide better mechanical strength and flexibility for Pb^{2+} response, their large scales in 2D/3D

Received: April 27, 2013
Accepted: July 8, 2013
Published: July 8, 2013

 © 2013 American Chemical Society dx.doi.org/10.1021/am401570k | ACS Appl. Mater. Interfaces 2013, 5, 7219−7226

dimensions limit their application in microenvironments. Recently developed microfluidics[36−40] can miniaturize these systems to microscale to achieve faster response.[41] On the basis of the microfluidic technique, hollow poly(NIPAM-*co*-B18C6Am) microcapsules with Pb^{2+}-responsive volume change have been prepared.[42] However, lack of remote-controlled locomotion limits their further use for wireless manipulation in microenvironment. Therefore, development of microscale actuators with remote-controlled locomotion and fast Pb^{2+}-responsive volume changes is still highly required for micromanipulation in Pb^{2+}-contaminated microenvironments.

Recently developed multicomponent multiple emulsions from microfluidics[43,44] offer a versatile and promising platform for incorporating different functional components into a single entity for design and fabrication of microscale multifunctional systems with controlled structures. On the basis of this technique, here we report on a novel poly(NIPAM-*co*-B18C6Am) (PNB) microactuator with fast Pb^{2+}-response and remotely controlled magnetic-guided locomotion for micromanipulation such as preventing leaking of Pb^{2+}-contaminated solution from microchannel or microcrack. The PNB microactuators are prepared from quadruple-component double emulsion templates, each with a soybean oil droplet (O_1) and a ferrofluid droplet (O_2) in a water drop (W), which is then dispersed in an oil phase (O) to form (O_1+O_2)/W/O double emulsions. The O_1 phase is used for constructing a hollow cavity and the O_2 phase is used for fabricating an eccentric magnetic core inside the microactuator. In the PNB shell of microactuators, the B18C6Am moieties work as sensors for Pb^{2+} recognization, whereas the PNIPAM networks act as actuators for swelling/shrinking volume change based on Pb^{2+} recognization. The eccentric magnetic core enables translational and rotational motion of the microactuators under magnetic guide for remote-control. The inner cavity provides larger surface area and less resistance for transport of Pb^{2+}-contaminated solution in the microactuator, which leads to a fast Pb^{2+}-response rate. Under magnetic guide, the microactuators can be quickly and precisely transported to the desired site where Pb^{2+} leaks; and then they clog the leaking microchannel or microcrack with Pb^{2+}-responsive volume swelling to prevent flowing out of Pb^{2+}-contaminated solution.

EXPERIMENTAL SECTION

Materials. NIPAM (Sigma-Aldrich) was purified by recrystallization with a hexane/acetone mixture (v/v, 50/50). B18C6Am was synthesized according to literatures.[45,46] *N*,*N*′-Methylenebisacrylamide (MBA) was used as the cross-linker. 2,2′-Azobis(2-amidi-nopropane dihydrochloride) (V50) and 2,2-dimethoxy-2-phenylacetophenone (BDK) were respectively used as the initiators dissolved in aqueous phase and oil phase. Pluronic F-127 (Sigma-Aldrich) and polyglycerol polyricinoleate (PGPR 90) (Danisco, Denmark) were respectively used as the emulsifiers for aqueous phase and oil phase. All other reagents were of analytical grade and used as received. Lead nitrate was dissolved in deionized (DI) water as the heavy metal source. DI water from a Milli-Q Plus water purification system (Millipore) was used throughout the experiments.

Microfluidic Device. Capillary microfluidic device was fabricated by assembling glass capillary tubes on glass slides,[36,37,43] as illustrated in Figure 1a. The inner dimension of square capillary tubes (AIT glass) and outer diameter of cylindrical capillaries (Vitrocom) were 1.0 mm. The inner diameters of the injection tube 1, injection tube 2, connection tube 1, connection tube 2, transition tube, and collection tube were 580, 580, 150, 150, 250, and 500 μm, respectively. The front-ends of injection tube 1, injection tube 2, and transition tube were tapered by a micropuller (Narishige) and then adjusted by a microforge (Narishige) with inner diameters at 50, 50, and 180 μm, respectively. All cylindrical capillaries were coaxially aligned within the square capillary tubes by matching the outer diameters of the cylindrical tubes to the inner dimensions of the square ones. The tapered end of the injection tubes were inserted into the connection tubes, which were then linked with the transition tube to form a Y-shaped connector; then the outlet of the transition tube was inserted into the collection tube to fabricate the microfluidic device.

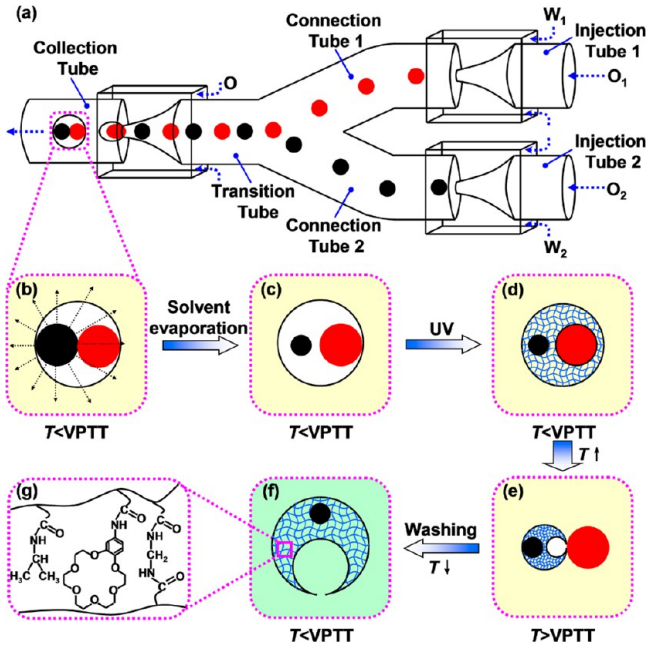

Figure 1. Schematic illustration of the fabrication process of PNB microactuators. (a) Microfluidic device for generating (O_1+O_2)/W/O double emulsions. (b, c) Solvent evaporation process for constructing the magnetic PS core. (d−g) (d) UV-initiated polymerization of emulsion templates followed by (e) releasing the soybean oil core by heating for (f) fabricating PNB microactuators with (g) cross-linked polymeric shell.

Preparation of Poly(NIPAM-*co*-B18C6Am) Microactuators. First, for constructing the magnetic core in the microactuator, oleic-acid-modified magnetic nanoparticles (OA-MNPs) were prepared by using coprecipitation method.[47−49] Briefly, hydrochloric acid (4 mL) and $FeCl_2{\cdot}4H_2O$ (7.2 g) were dissolved into DI water (20 mL). The resultant solution was mixed with aqueous solution of $FeCl_3{\cdot}6H_2O$ (29 mL, 27 wt %) and followed with addition of DI water (47 mL). Then, ammonia (40 mL, 25 wt %) was added under vigorous agitation. The solution immediately turned to dark, indicating that the magnetic nanoparticles (MNPs) were synthesized. After reaction for 20 min, the obtained MNPs were washed with DI water repeatedly and separated by a magnet. Oleic acid (OA) (6 g), which was preheated at 60 °C for 5−10 min, was added into the MNPs drop by drop and mixed at 60 °C for another 20 min. The obtained OA-MNPs were washed by ethanol (100 mL) to remove the excess OA, and then separated by a magnet. Ferrofluid was obtained by adding n-hexane into the OA-MNPs dropwise under stirring.

The microactuators were prepared from quadruple-component (O_1+O_2)/W/O double emulsions. UV-initiated polymerization was employed to convert the monomer-containing middle aqueous layer into the hydrogel body of the microactuator. To construct the inner magnetic core, we used volatile organic solvent as the carrying fluid for MNPs to form homogeneous and stable ferrofluid; because the microfluidic fabrication usually requires homogeneously and stably dispersed nanoparticles inside the droplets for preventing clogging. The organic solvent can dissolve a range of polymers for constructing the solid magnetic core by solvent evaporation. Moreover, combination of the UV-initiated polymerization and solvent evaporation in the emulsion system to respectively fabricate the

hydrogel shell and magnetic core of the microactuators also highlights the flexibility of our fabrication strategy.

Typically, soybean oil (10 mL) containing PGPR 90 (0.20 g, 2% (w/v)), BDK (0.10 g, 1% (w/v)), and Sudan III (0.0050 g, 0.05% (w/v)) was used as the inner oil phase 1 (O_1). Isopentyl acetate (10 mL) with polystyrene (PS) (0.50 g, 5% (w/v)) and ferrofluid (2 mL, 20% (v/v)) was used as the inner oil phase 2 (O_2). NIPAM (0.6780 g, 1 mol/L), B18C6Am (0.2286 g, 0.1 mol/L), MBA (0.0185 g, 0.02 mol/L), Pluronic F-127 (0.06 g, 1 wt %), V50 (0.03 g, 0.5 wt %), and glycerin (0.36 g, 6 wt %) were dissolved in DI water (6 mL) as the middle aqueous phase (W). Soybean oil (100 mL) containing PGPR 90 (10 g, 10% (w/v)) and BDK (1 g, 1% (w/v)) was used as the outer oil phase (O). To fabricate the (O_1+O_2)/W/O double emulsions, we first emulsified two different inner oil phases (O_1 and O_2) separately by middle aqueous phase at the tip of injection tube 1 and 2 to generate monodisperse oil droplets. Then, through the connection tubes, these two sets of droplets flowed into the transition tube, where they were merged to form a linear array of droplets in the middle aqueous phase. The middle aqueous phase was further emulsified by the outer oil phase in the collection tube downstream, forming quadruple-component (O_1+O_2)/W/O double emulsions containing two different droplets (Figure 1a). The fluid phases were pumped into the microfluidic device by syringe pumps, with flow rates of $Q_{O1} = Q_{O2} = 100\ \mu L/h$, $Q_{W1} = 400\ \mu L/h$, $Q_{W2} = 500\ \mu L/h$, and $Q_O = 6000\ \mu L/h$, respectively. The obtained (O_1+O_2)/W/O double emulsions were collected in a Petri dish containing soybean oil with 10% (w/v) PGPR 90 and 1% (w/v) BDK (Figure 1b). Then, the obtained emulsions were kept for 40 min to allow evaporation of the isopentyl acetate and n-hexane in the ferrofluid droplet (O_2) for constructing the solid magnetic PS core (Figure 1c). The middle aqueous phase of the double emulsions was converted into hydrogel by UV irradiation for 15 min in an ice−water bath to keep the reaction temperature lower than the lower critical solution temperature (LCST) of PNIPAM. A 250 W UV lamp with an illuminance spectrum of 250−450 nm was employed to produce UV light. Under UV light, the activated photoinitiator BDK diffused to the interface between the outer oil phase and middle aqueous phase, where it triggered the polymerization of NIPAM and B18C6Am in the middle aqueous phase to build PNB microgel. The soybean oil droplet and magnetic core were encapsulated inside the microgel after polymerization (Figure 1d). Then, by heating to 65 °C, the inner soybean oil droplet was squeezed out of the microgel, resulting in a cavity in the microactuator and a cracked hole in the shell (Figure 1e). After washing with DI water, PNB microactuators each with a cavity and an eccentric magnetic core were obtained (Figure 1f). The chemical structure of the cross-linked PNB networks of the microactuators was illustrated in Figure 1g.

Characterization. The morphology and size of OA-MNPs were characterized by transmission electron microscopy (TEM, JEM-100CX, JEOL), with an acceleration voltage of 80 kV. TEM sample was prepared by dripping a drop of alcoholic dispersion of OA-MNPs onto a copper grid. (O_1+O_2)/W/O double emulsions formation was observed by an inverted optical microscope (IX71, Olympus) and recorded by a high speed digital camera (Phantom Miro3, Vision Research). Optical microscope images of the (O_1+O_2)/W/O double emulsions and microactuators were obtained by an optical microscope (BX 61, Olympus). The size and size distribution of the samples were determined based on their optical micrographs using automatic analytic software. The chemical structure of the PNB microactuators was characterized by Fourier Transform Infrared Spectroscope (FT-IR, IR prestige-21, Shimazu) in the range of 4000−400 cm^{-1} with KBr disc technique. The sample for FT-IR characterization was prepared by a freeze-drying method.

Magnetic-guided targeting behavior of the PNB microactuator was performed in a glass holder (size: Ø 6 mm) with a T-shaped channel containing aqueous solution with 0.4 wt % bovine serum albumin (BSA) at 41.2 °C. A cylindrical NdFeB magnet (size: Ø 4 mm ×10 mm) with the central magnetic intensity of 1.2 T was used to guide the microactuator movement, as measured by a Digital teslameter (STI-2T, Mianyang New Asia Technology Co., Ltd.). The thermoresponsive volume changes of PNB microactuators in DI water and 0.02 mol/L Pb^{2+} aqueous solution were investigated to study the Pb^{2+}-responsive behaviors. The temperature range was selected from 19 to 60 °C. At each temperature, the samples were equilibrated at least 15 min to reach their equilibrium state. PNIPAM microactuators were used as the control group (see the Supporting Information for the preparation of PNIPAM microactuators). To investigate the effect of cavity on the response rate, we studied the dynamic swelling behaviors of PNB microactuators and voidless PNB microspheres at 40.4 °C upon addition of 0.02 mol/L Pb^{2+}. Micromanipulation of the PNB microactuator for preventing Pb^{2+} leakage from microchannel or microcrack was performed in a tapered microtube that was inserted in a square one. Aqueous solution of 0.1 wt % BSA was used as the medium. The temperature was set at 41.8 °C to keep the microactuator in a shrinking state. Briefly, the microactuator was first moved into the microtube by an external magnetic guide. Then, aqueous solution containing 0.02 mol/L Pb^{2+} ion was flowed out of the microtube to induce swell of the microactuator to clog the microtube. All of these characterizations were observed and recorded by an optical microscope equipped with a thermostatic stage system (TS 62, Instec, USA) and a CCD camera.

RESULTS AND DISCUSSION

Fabrication of Monodisperse (O_1+O_2)/W/O Double Emulsions and Poly(NIPAM-*co*-B18C6Am) Microactuators. For template synthesis of PNB microactuators, monodisperse (O_1+O_2)/W/O double emulsions, each with a red oil droplet and a black ferrofluid droplet, are generated from the microfluidic device (Figure 2a and Movie S1 in the Supporting Information). The mean diameter of the OA-MNPs dispersed in inner ferrofluid droplet is ∼12 nm, as shown in the TEM image of Figure 2b. The generated double emulsions are then collected in a vessel and kept for 40 min to allow solvent evaporation of the isopentyl acetate in the ferrofluid droplet; this results in decreasing size of the ferrofluid droplet and precipitation of the contained PS polymers and OA-MNPs for forming solid magnetic PS core in the double emulsions (Figure 2c). Figure 2d shows the size decrease of the ferrofluid droplet during the solvent evaporation process, where V_t and V_0 respectively represent the evolved volumes at time t and at the beginning. The results show a fast solvent evaporation process for producing the solid magnetic core. The size distributions of emulsion templates during the period of t = 405−475 s are shown in Figure 2e, with d_o, d_1, and d_2 respectively representing the diameters of the (O_1+O_2)/W/O double emulsions, the inner soybean oil droplets, and the inner ferrofluid droplets. The average diameters of d_o, d_1, and d_2 are 356, 179, and 123 μm, respectively. The coefficient of variation (CV), which is defined as the ratio of the standard deviation of the size distribution to its arithmetic mean, is used to characterize the size monodispersity of the emulsion templates. The CV values of d_o, d_1, and d_2 are 1.3, 1.6, and 2.3%, respectively, indicating good monodispersity of the emulsion templates. After UV-initiated polymerization of the emulsion templates and removal of the red soybean oil droplet by heating, PNB microactuators are prepared. The inserted optical micrograph of PNB microactuator from the emulsion templates (Figure 2c) in DI water at 19.8 °C clearly shows the eccentric magnetic core and hollow cavity structure. The FT-IR characterization results confirm the chemical composition of the PNB shell of microactuators (see Figures S1 and S2 in the Supporting Information).

Magnetic-Guided Targeting Behavior of Poly(NIPAM-*co*-B18C6Am) Microactuators. The OA-MNPs embedded in the PS core allow wireless manipulation of the microactuators with an external magnetic field. With this eccentric magnetic PS

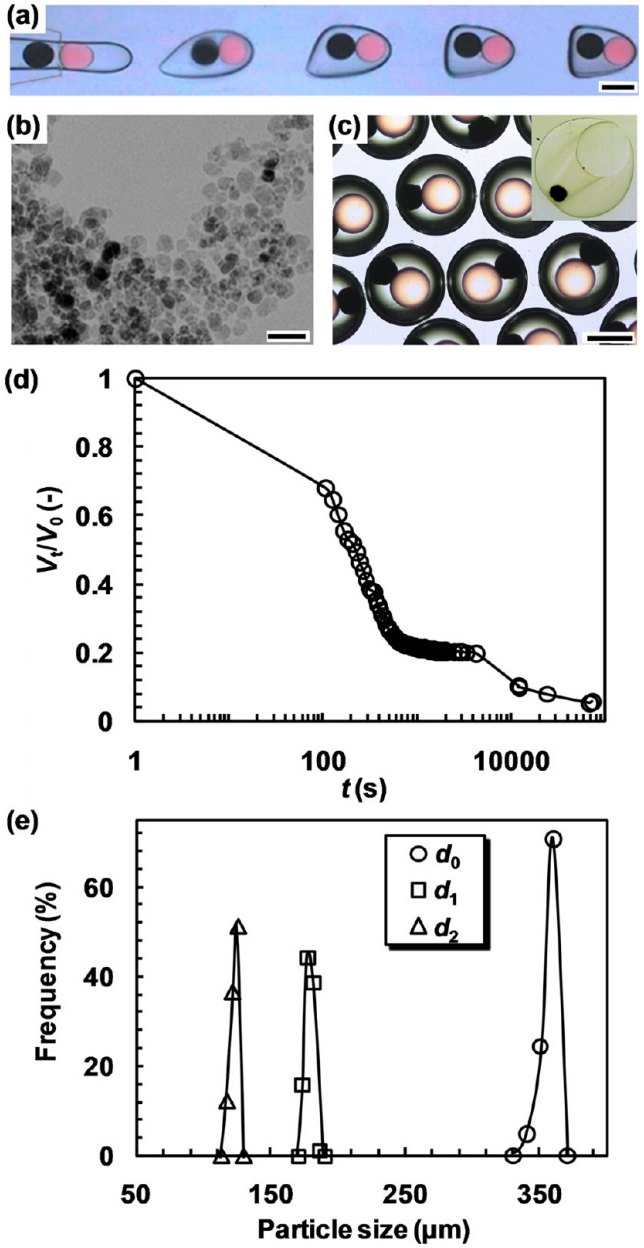

Figure 2. Template synthesis of PNB microactuators from quadruple-component (O_1+O_2)/W/O double emulsions. (a) High-speed optical micrograph showing the generation of double emulsions in microfluidic device. (b) TEM image of oleic-acid-modified magnetic nanoparticles. (c) Optical micrograph of the double emulsions at 425 s after formation and the resultant PNB microactuator (inserted image) at 19.8 °C in DI water. (d) The time-dependent volume change of the magnetic droplet, where V_t and V_0 are respectively the droplet volumes at time t and that at the beginning. (e) Size distributions of the double emulsions during t = 405−475 s, where d_0, d_1, and d_2 are respectively the diameters of the double emulsions, the inner soybean oil droplets and the inner ferrofluid droplets. Scale bars in a and c are 200 μm, and that in b is 30 nm.

core, the PNB microactuator enables not only translational motion but also rotational motion. The magnetic-guided movement of the microactuator is carried out in a glass holder with a T-shaped channel (Figure 3 and Movie S2 in the Supporting Information). A magnet was placed near the glass holder and moved manually to guide the movement of the microactuator (Figure 3a). Aqueous solution containing 0.4 wt % BSA was used in the glass holder to prevent adhesion of the microgel actuator on the glass surfaces (see Figure S3 in the Supporting Information for the effect of BSA on the thermo-response of PNB microactuators).[50,51] Under magnetic-guide, the PNB microactuator placed at the top of the channel can move through every corner of the T-shaped channel via rotational and directed movement (Figure 3b−i). The magnetic intensity to induce the microactuator movement was about 0.08 T. Because the magnetic response can be enhanced by using magnetic field with higher intensity or using magnetic core with more magnetic nanoparticles, the power for driving the actuation and rotation can be easily adjusted. Such a magnetic-responsive property can make the microactuators achieve the purpose of site- and/or route-specific targeting behaviors, with the accuracy depending on the precise manipulation of the external magnetic field.[52,53]

Effects of Pb^{2+} on the Thermoresponsive Volume Change Behaviors of Poly(NIPAM-*co*-B18C6Am) Microactuators. The effect of Pb^{2+} on the thermo-responsive volume change behaviors of the PNB microactuators is studied by using PNIPAM microactuators as the control group. The thermo-responsive volume changes of PNB and PNIPAM microactuators in DI water and 0.02 mol/L Pb^{2+} aqueous solution are plotted in Figure 4 (see Figures S4−S6 in the Supporting Information for the preparation of PNIPAM microactuators, the effect of cross-linker fraction on the thermo-responsive property and optical micrographs of PNB and PNIPAM microactuators in deionized water and 0.02 mol/L Pb^{2+} solution). V_T and V_0 are respectively the volume of microactuators at a certain temperature and that at the initial temperature (~19 °C). VR_1 and VR_2 are respectively the volume ratios (V_T/V_0) for the microactuators and the inner cavity. The volumes of all microactuators decrease with increasing temperature, showing excellent thermo-responsive properties. The temperature, at which the value of V_T/V_0 decreases to half of the total change value, is taken as the LCST of the microactuator. The PNIPAM microactuators in both solutions show similar volume change behaviors with LCST ≈ 31 °C (Figure 4a, c), which is in agreement with the value reported in literatures.[24] By contrast, PNB microactuators exhibit a thermo-responsive volume change behavior with a higher LCST in 0.02 mol/L Pb^{2+} aqueous solution ($LCST_2$ ≈ 47 °C) than that in DI water ($LCST_1$ ≈ 31.5 °C) (Figure 4b, c). The different behaviors of PNB microactuators are due to the formation of crown ether/Pb^{2+} ions complexes in the hydrogel polymeric networks. The host compound, B18C6Am moieties can selectively capture the guest Pb^{2+} ions into their cavities through supramolecular "host-guest" complexation. These complexes cause charged polymer chains inside the cross-linked microactuator, which produces repulsion force among each other and results in osmotic pressure to resist the shrinking of PNB networks during increasing temperature. Thus, more swollen PNB microactuators are obtained in 0.02 mol/L Pb^{2+} aqueous solution, leading to an increased LCST. To achieve isothermal Pb^{2+}-induced volume swell of the PNB microactuators, the optimal operating temperature should locate between the $LCST_1$ (31.5 °C) and $LCST_2$ (47 °C).

To evaluate the optimal operation temperature, a parameter defined as $V\mathrm{Pb}^{2+}/V\mathrm{H_2O}$ is introduced, where $V\mathrm{Pb}^{2+}$ and $V\mathrm{H_2O}$ are respectively the average volumes of PNB microactuators in 0.02 mol/L Pb^{2+} aqueous solution and DI water at each temperature (Figure 4d). With increasing the temperature, the $V\mathrm{Pb}^{2+}/V\mathrm{H_2O}$ value increases at first, and then decreases. The

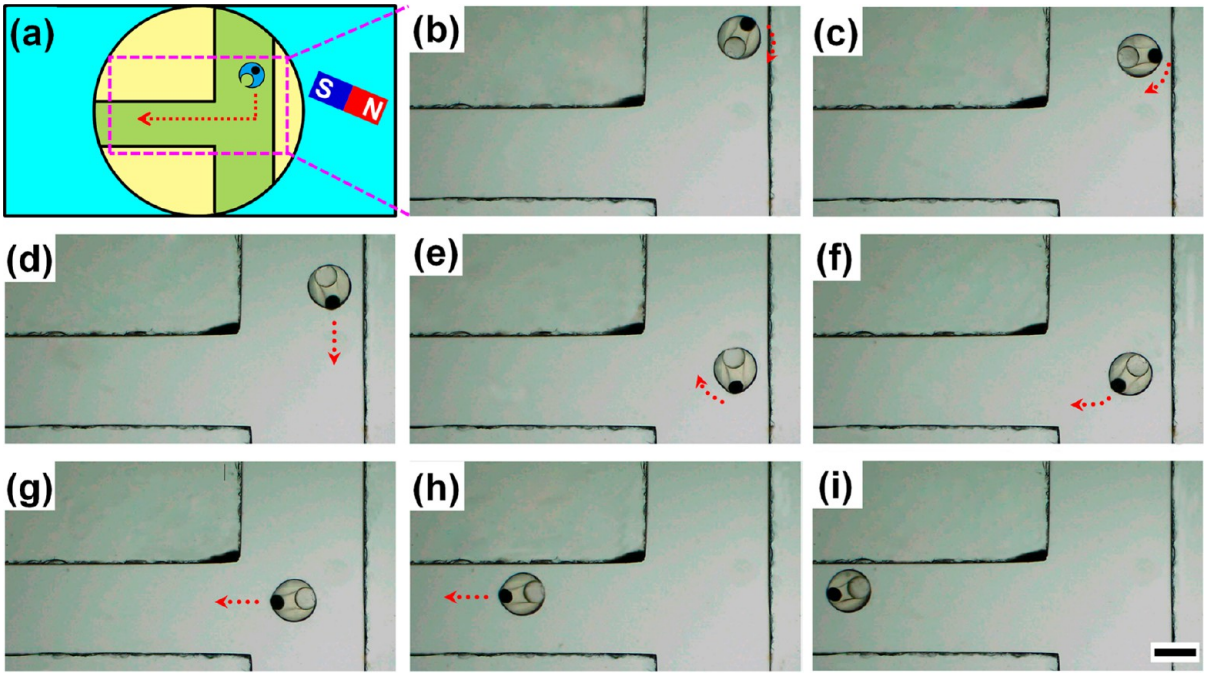

Figure 3. Magnetic-guided movement of the PNB microactuator. (a) Scheme illustrating the experimental setup. (b–i) Optical micrographs showing the magnetic-guided movement of a PNB microactuator in aqueous solution containing 0.4 wt % BSA at 41.2 °C. Scale bar is 200 μm.

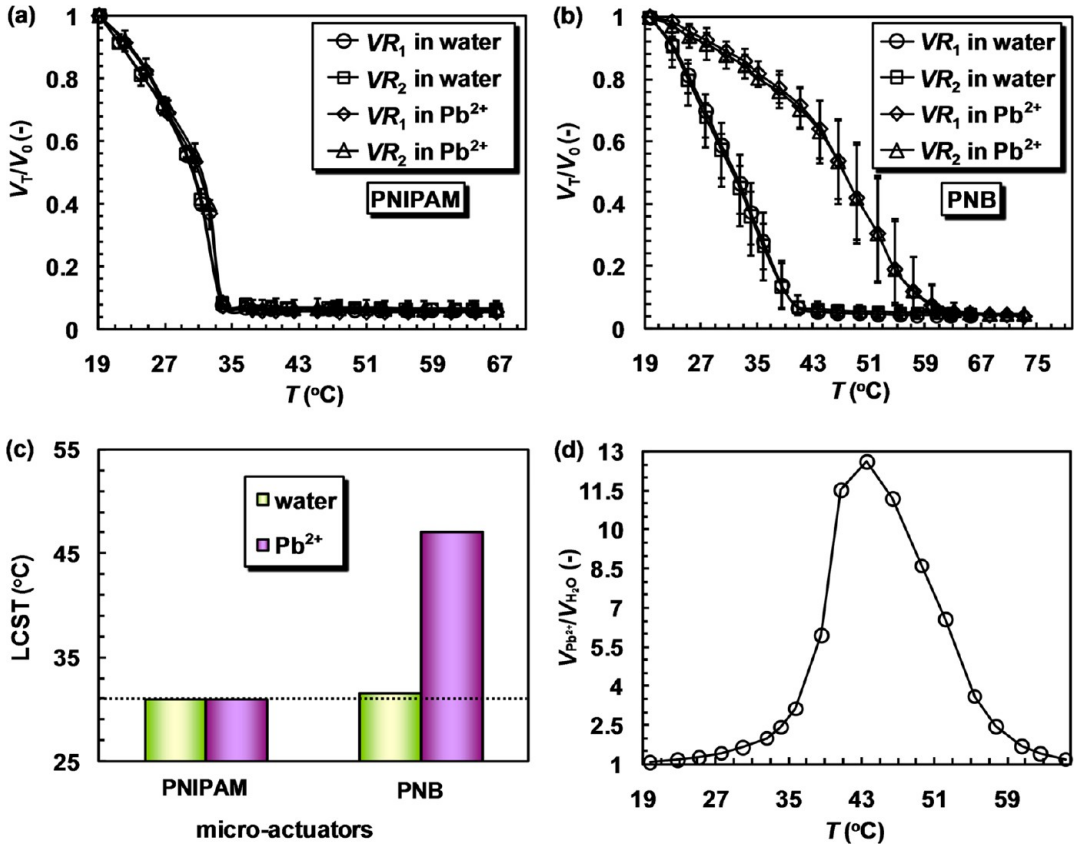

Figure 4. Deswelling behaviors of (a) PNIPAM and (b) PNB microactuators, where V_T and V_0 are respectively the equilibrium volumes at temperature T and that at the initial temperature (19 °C), and VR_1 and VR_2 represent the volume ratio (V_T/V_0) for the microactuators and the inner cavity, respectively. (c) LCST of PNIPAM and PNB microactuators in DI water and Pb^{2+} aqueous solution. (d) Temperature-dependent volume change ratio of PNB microactuators in Pb^{2+} aqueous solution to that in DI water. The concentration of Pb^{2+} is 0.02 mol/L.

maximum value of VPb^{2+}/VH_2O is obtained at 43.6 °C, which indicates the optimal operation temperature for the PNB microactuators to achieve the best Pb^{2+}-responsive property is around 43.6 °C.

dx.doi.org/10.1021/am401570k | ACS Appl. Mater. Interfaces 2013, 5, 7219–7226

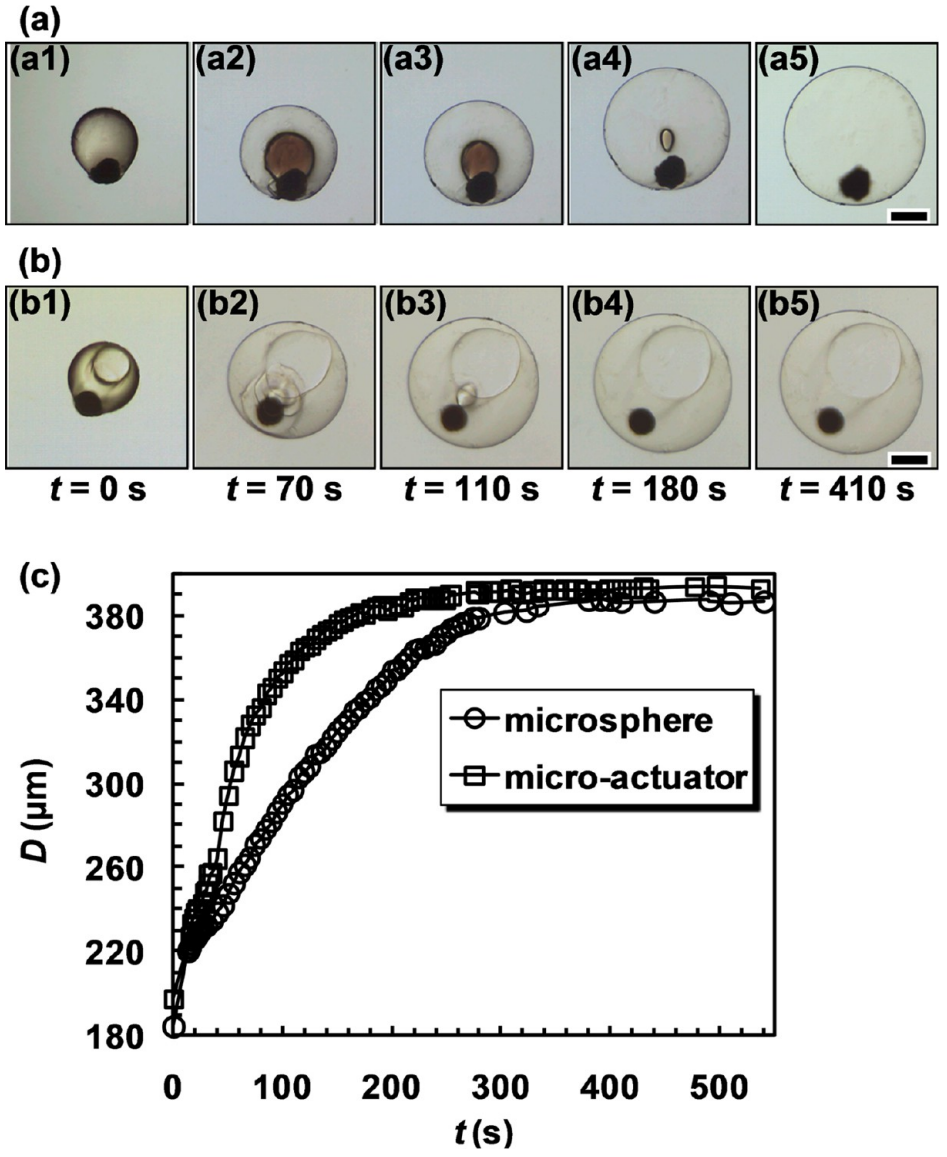

Figure 5. Optical micrographs of the Pb^{2+}-induced swelling behaviors of (a) voidless PNB microsphere and (b) PNB microactuator, where *t* represents the time right after addition of 0.02 mol/L Pb^{2+}. (c) Dynamic diameter changes of voidless PNB microsphere and microactuator upon addition of 0.02 mol/L Pb^{2+}. Temperature is 40.4 °C. Scale bars are 100 μm.

Effects of Hollow Cavity on the Time-dependent Volume Change Behaviors of Poly(NIPAM-*co*-B18C6Am) Microactuators. The effect of hollow cavity on the time-dependent volume change behavior of the PNB microactuator is studied by using voidless PNB microsphere with the same diameter as the control group. As shown in Figure 5, the PNB microactuator and voidless microsphere are both in shrink states in DI water at 40.4 °C (t = 0 s). Upon addition of 0.02 mol/L Pb^{2+}, PNB microactuator (Figure 5b) exhibits a much faster swelling process than the voidless microsphere (Figure 5a). Because the surface part contacts Pb^{2+} first, it swells earlier than the central part. This nonuniform swelling leads to the central part with worse transmittance, and thus a dark area is observed for the shrinking central part (Figure 5a).

The time-dependent diameter changes of the microactuator and voidless microsphere are plotted in Figure 5c. Upon addition of 0.02 mol/L Pb^{2+}, the diameter of PNB micro-actuator increases faster than that of the voidless microsphere during the first ~220 s, and reaches same value at t = ~400 s. It is reported that the response rate of cross-linked microgel is governed by diffusion-limited transport of water molecules in and out of the cross-linked networks.[54] Thus, compared with the voidless structure of PNB microsphere, the hollow cavity together with the hole structure in the shell would provide the microactuator with larger surface area and much less resistance for transporting Pb^{2+} ions, which leads to faster Pb^{2+}-response rate of PNB microactuator.

Micromanipulation of Poly(NIPAM-*co*-B18C6Am) Microactuators for Preventing Pb^{2+} Leakage from Microtube. The application of these PNB microactuators for micromanipulation in microenvironment is demonstrated by using them to prevent Pb^{2+} leaking from microtube with Pb^{2+}-contaminated solution flowing through (Figure 6). One-tenth weight percent BSA was added into the aqueous solution to prevent the adhesion of the microactuators on the glass surface to achieve a smooth magnetic-guided movement.[50,51] Meanwhile, the BSA can also serve as an indicator to indicate the inflow of Pb^{2+} solution because of the formation of visible

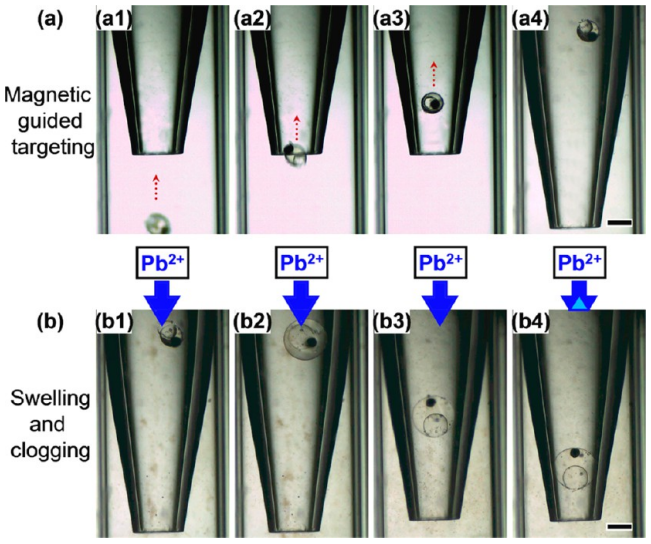

Figure 6. Micromanipulation of PNB microactuator for preventing Pb^{2+} leakage from microtube. (a) Magnetic-guided targeting process of the microactuator into the microtube. (b) Clogging of the microtube by Pb^{2+}-responsive swelling of the microactuator in response to flow of Pb^{2+}-contaminated solution. Scale bars are 200 μm.

precipitation when BSA contacts with Pb^{2+} (Figure 6b). First, under magnetic-guide, the PNB microactuator with an initial shrinking state is moved into the tapered microtube with inner diameter of the tip at 260 μm (Figure 6a1–a4). When aqueous solution containing Pb^{2+} flows through the microtube, the Pb^{2+}-responsive microactuator isothermally swells due to the repulsion among charged BCAm/Pb^{2+} complex and the osmotic pressure within the polymeric networks (Figure 6b1, b2). Then, the microactuator is moved to the microtube tip, and clogs the microchannel with its swollen volume to prevent the Pb^{2+}-contaminated solution flowing out (Figure 6b3, b4). The demonstration results show that the microactuator shows excellent maneuverability and fast Pb^{2+}-response as micromanipulation system in Pb^{2+}-contaminated microenvironment in this study. Moreover, because microactuators with controlled sizes as well as size distributions can be fabricated from the microfluidic technique, which enables microactuators with a known size range can cover leaking microchannels with different sizes for practical applications.

CONCLUSIONS

In summary, PNB microactuators, each with an eccentric magnetic core and a hollow cavity, which enable remote-controlled locomotion and fast Pb^{2+}-response for micromanipulation in Pb^{2+}-contaminated microenvironment, have been successfully fabricated from quadruple-component double emulsions. The PNB shell acts as sensor and actuator for providing the microactuator with Pb^{2+}-responsive volume change function. The eccentric magnetic core enables magnetic manipulation of the microactuator for site- and/or route-specific targeting. The inner cavity and cracked hole in the shell offer larger surface area and less resistance for transporting Pb^{2+} ions into the polymeric shell networks to achieve a fast Pb^{2+}-response rate. The micromanipulation of the microactuators in Pb^{2+}-contaminated microenvironment is demonstrated by first transporting them to a desired Pb^{2+}-leaking site precisely under magnetic-guide, and then preventing Pb^{2+}-leakage from a microchannel via the Pb^{2+}-induced isothermal volume-swelling. Moreover, by simply changing the shell materials, microactuators that are responsive to other stimuli such as pH and other ions can be developed. The proposed microactuators offer a novel and promising platform for design and fabrication of multifunctional actuators and sensors, biomimetic soft microrobots, microelectro-mechanical systems, and drug delivery systems.

ASSOCIATED CONTENT

Supporting Information

FT-IR spectra of B18C6Am and PNB microactuators, effect of BSA aqueous solution on the thermo-response of PNB microactuators, optical micrographs of the PNIPAM microactuators and emulsion templates, effect of cross-linker fraction on the thermoresponse of PNIPAM microactuators, effect of Pb^{2+} on the thermoresponsive volume change behaviors of PNIPAM and PNB microactuators, high-speed movie showing generation of double emulsions, and movie showing the magnetic-guided movement of a PNB microactuator. This material is available free of charge via the Internet at http://pubs.acs.org/.

AUTHOR INFORMATION

Corresponding Author

*Corresponding Authors E-mail: chuly@scu.edu.cn (L.Y.C.), wangwei512@scu.edu.cn (W.W.).

Notes

The authors declare no competing financial interest.

ACKNOWLEDGMENTS

The authors gratefully acknowledge support from the National Natural Science Foundation of China (21136006), the Program for Changjiang Scholars and Innovative Research Team in University (IRT1163), and the State Key Laboratory of Polymer Materials Engineering (Sichuan University).

REFERENCES

(1) Kim, J.; Hanna, J. A.; Byun, M.; Santangelo, C. D.; Hayward, R. C. *Science* **2012**, *335*, 1201–1205.
(2) Yeghiazarian, L.; Arora, H.; Nistor, V.; Montemagno, C.; Wiesner, U. *Soft Matter* **2007**, *3*, 939–944.
(3) Wang, W.; Yao, C.; Zhang, M. J.; Ju, X. J.; Xie, R.; Chu, L. Y. *J. Phys. D: Appl. Phys.* **2013**, *46*, 114007.
(4) Zhang, N.; Li, R.; Zhang, L.; Chen, H.; Wang, W.; Liu, Y.; Wu, T.; Wang, X.; Wang, W.; Li, Y.; Zhao, Y.; Gao, J. *Soft Matter* **2011**, *7*, 7231–7239.
(5) Stuart, M. A. C.; Huck, W. T. S.; Genzer, J.; Müller, M.; Ober, C.; Stamm, M.; Sukhorukov, G. B.; Szleifer, I.; Tsukruk, V. V.; Urban, M.; Winnik, F.; Zauscher, S.; Luzinov, I.; Minko, S. *Nat. Mater.* **2010**, *9*, 101–113.
(6) Ma, Y.; Zhang, Y.; Wu, B.; Sun, W.; Li, Z.; Sun, J. *Angew. Chem., Int. Ed.* **2011**, *50*, 6254–6257.
(7) Ma, M.; Guo, L.; Anderson, D. G.; Langer, R. *Science* **2013**, *339*, 186–189.
(8) Maeda, S.; Hara, Y.; Sakai, T.; Yoshida, R.; Hashimoto, S. *Adv. Mater.* **2007**, *19*, 3480–3484.
(9) Kim, H. N.; Ren, W. X.; Kim, J. S.; Yoon, J. *Chem. Soc. Rev.* **2012**, *41*, 3210–3244.
(10) Goyer, R. A. *Environ. Health Perspect.* **1993**, *100*, 177–187.
(11) Gupta, S.; Kumar, D.; Gaur, J. P. *Chem. Eng. J.* **2009**, *148*, 226–233.
(12) Shen, X. M.; Rosen, J. F.; Guo, D.; Wu, S. M. *Sci. Total Environ.* **1996**, *181*, 101–109.
(13) Zamani, A. A.; Khorsihdi, N.; Mofidi, Z.; Yaftian, M. R. *J. Chin. Chem. Soc.* **2011**, *58*, 673–680.

(14) Parra, E. J.; Blondeau, P.; Crespo, G. A.; Rius, F. X. *Chem. Commun.* **2011**, *47*, 2438−2440.
(15) Srivastava, S. K.; Gupta, V. K.; Jain, S. *Analyst* **1995**, *120*, 495−498.
(16) Pan, X.; Wang, Y.; Jiang, H.; Zou, G.; Zhang, Q. *J. Mater. Chem.* **2011**, *21*, 3604−3610.
(17) Xia, W. S.; Schmehl, R. H.; Li, C. J.; Mague, J. T.; Luo, C. P.; Guldi, D. M. *J. Phys. Chem. B* **2002**, *106*, 833−843.
(18) Yu, M.; He, F.; Tang, Y.; Wang, S.; Li, Y.; Zhu, D. *Macromol. Rapid Commun.* **2007**, *28*, 1333−1338.
(19) Sasaki, D. Y.; Waggoner, T. A.; Last, J. A.; Alam, T. M. *Langmuir* **2002**, *18*, 3714−3721.
(20) Luo, Q.; Guan, Y.; Zhang, Y.; Siddiq, M. *J. Polym. Sci., Part A: Polym. Chem.* **2010**, *48*, 4120−4127.
(21) Zhang, B.; Ju, X. J.; Xie, R.; Liu, Z.; Pi, S. W.; Chu, L. Y. *J. Phys. Chem. B* **2012**, *116*, 5527−5536.
(22) Izatt, R. M.; Pawlak, K.; Bradshaw, J. S.; Bruening, R. L. *Chem. Rev.* **1991**, *91*, 1721−2085.
(23) Scarpa, J. S.; Mueller, D. D.; Klotz, I. M. *J. Am. Chem. Soc.* **1967**, *89*, 6024−6030.
(24) Katayama, S.; Hirokawa, Y.; Tanaka, T. *Macromolecules* **1984**, *17*, 2641−2643.
(25) Chu, L. Y.; Yamaguchi, T.; Nakao, S. *Adv. Mater.* **2002**, *14*, 386−389.
(26) Yamaguchi, T.; Ito, T.; Sato, T.; Shinbo, T.; Nakao, S. *J. Am. Chem. Soc.* **1999**, *121*, 4078−4079.
(27) Ito, T.; Yamaguchi, T. *Angew. Chem., Int. Ed.* **2006**, *45*, 5630−5633.
(28) Ito, T.; Hioki, T.; Yamaguchi, T.; Shinbo, T.; Nakao, S.; Kimura, S. *J. Am. Chem. Soc.* **2002**, *124*, 7840−7846.
(29) Holtz, J. H.; Asher, S. A. *Nature* **1997**, *389*, 829−832.
(30) Holtz, J. H.; Holtz, J. S. W.; Munro, C. H.; Asher, S. A. *Anal. Chem.* **1998**, *70*, 780−791.
(31) Asher, S. A.; Peteu, S. F.; Reese, C. E.; Lin, M. X.; Finegold, D. *Anal. Bioanal. Chem.* **2002**, *373*, 632−638.
(32) Reese, C. E.; Asher, S. A. *Anal. Chem.* **2003**, *75*, 3915−3918.
(33) Liu, K.; Ji, H. F. *Anal. Sci.* **2004**, *20*, 9−11.
(34) Geary, C. D.; Zudans, I.; Goponenko, A. V.; Asher, S. A.; Weber, S. G. *Anal. Chem.* **2005**, *77*, 185−192.
(35) Ju, X. J.; Zhang, S. B.; Zhou, M. Y.; Xie, R.; Yang, L.; Chu, L. Y. *J. Hazard. Mater.* **2009**, *167*, 114−118.
(36) Utada, A. S.; Lorenceau, E.; Link, D. R.; Kaplan, P. D.; Stone, H. A.; Weitz, D. A. *Science* **2005**, *308*, 537−541.
(37) Chu, L. Y.; Utada, A. S.; Shah, R. K.; Kim, J. W.; Weitz, D. A. *Angew. Chem., Int. Ed.* **2007**, *46*, 8970−8974.
(38) Shah, R. K.; Shum, H. C.; Rowat, A. C.; Lee, D.; Agresti, J. J.; Utada, A. S.; Chu, L. Y.; Kim, J. W.; Fernandez-Nieves, A.; Martinez, C. J.; Weitz, D. A. *Mater. Today* **2008**, *11*, 18−27.
(39) Liu, L.; Wang, W.; Ju, X. J.; Xie, R.; Chu, L. Y. *Soft Matter* **2010**, *6*, 3759−3763.
(40) Liu, L.; Yang, J. P.; Ju, X. J.; Xie, R.; Liu, Y. M.; Wang, W.; Zhang, J. J.; Niu, C. H.; Chu, L. Y. *Soft Matter* **2011**, *7*, 4821−4827.
(41) Tanaka, T.; Fillmore, D. J. *J. Chem. Phys.* **1979**, *70*, 1214−1218.
(42) Pi, S. W.; Ju, X. J.; Wu, H. G.; Xie, R.; Chu, L. Y. *J. Colloid Interface Sci.* **2010**, *349*, 512−518.
(43) Wang, W.; Xie, R.; Ju, X. J.; Luo, T.; Liu, L.; Weitz, D. A.; Chu, L. Y. *Lab Chip* **2011**, *11*, 1587−1592.
(44) Wang, W.; Luo, T.; Ju, X. J.; Xie, R.; Liu, L.; Chu, L. Y. *Int. J. Nonlinear Sci. Numer. Simul.* **2012**, *13*, 325−331.
(45) Yagi, K.; Ruiz, J. A.; Sanchez, M. C. *Makromol. Chem., Rapid Commun.* **1980**, *1*, 263−268.
(46) Ungaro, R.; El Haj, B.; Smid, J. *J. Am. Chem. Soc.* **1976**, *98*, 5198−5202.
(47) MASSART, R. *IEEE Trans. Magn.* **1981**, *MAG-17*, 1247-1248.
(48) Wang, W.; Liu, L.; Ju, X. J.; Zerrouki, D.; Xie, R.; Yang, L.; Chu, L. Y. *ChemPhysChem* **2009**, *10*, 2405−2409.
(49) Omer, M.; Haider, S.; Park, S. Y. *Polymer* **2011**, *52*, 91−97.
(50) Wyss, H. M.; Franke, T.; Mele, E.; Weitz, D. A. *Soft Matter* **2010**, *6*, 4550−4555.
(51) Delamarche, E.; Bernard, A.; Schmid, H.; Bietsch, A.; Michel, B.; Biebuyck, H. *J. Am. Chem. Soc.* **1998**, *120*, 500−508.
(52) Chen, C. H.; Abate, A. R.; Lee, D.; Terentjev, E. M.; Weitz, D. A. *Adv. Mater.* **2009**, *21*, 3201−3204.
(53) Kim, S. H.; Sim, J. Y.; Lim, J. M.; Yang, S. M. *Angew. Chem., Int. Ed.* **2010**, *49*, 1−6.
(54) Chu, L. Y.; Kim, J. W.; Shah, R. K.; Weitz, D. A. *Adv. Funct. Mater.* **2007**, *17*, 3499−3504.